III. Algorithm Description

The method used in this search is a modified interval halving (binary search) algorithm. As the resonator tuner is comprised of two resonant cavities, the algorithm alternately tunes the resonant frequency of each cavity until the end condition of the search is met. For each of the resonant frequencies f_1 and f_2, a frequency range is specified to give the bounds of the optimization. The process of a single interval-halving iteration that is performed alternately for each resonant frequency is shown in Fig. 3. The algorithm first simulates the PAE at the midpoint frequency in the f_1 range (f_c) and at a neighboring point of slightly higher frequency ($f_c + f_n$). If the PAE at $f_c + f_n$ is greater than at f_c (Fig. 3(a)), the next candidate f_{next} is chosen at the midpoint between the current candidate and the maximum resonant frequency f_{max}. If instead the PAE at $f_c + f_n$ is lower than the PAE at f_c (Fig. 3(b)), the next candidate f_{next} is chosen between the current candidate and the minimum resonant frequency f_{min}. After one iteration of interval halving is performed in f_1, interval halving is performed on the other resonant frequency f_2 while holding f_1 constant. The interval halving is performed alternately between f_1 and f_2 until the current candidate point has less than 1% higher PAE than the previous candidate.

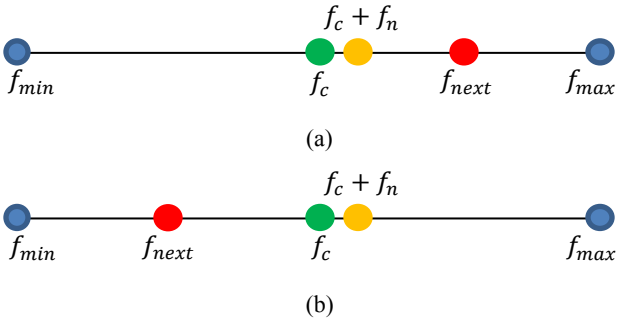

Fig. 3. Modified interval halving search algorithm. The resonant frequency of each tuner is alternately optimized to maximize PAE. Two cases exist: (a) the neighboring point has greater PAE than the starting point, and (b) the neighboring point has lower PAE than the starting point.

IV. Simulation Results

The algorithm was tested in simulation with tuner resonant frequency ranges of 3.05-3.57 GHz . A built-in field-effect transistor model was used in ADS to represent the transistor. The search shown in Fig. 4 gives a maximum PAE value of 44.93% at the resonant frequency combination of $f_1 = 3.20$ GHz, $f_2 = 3.47$ GHz. The candidate points of the search are shown in Fig. 5 as impedances on the Smith Chart. Figure 6 shows the traditional load-pull contours. Comparison of Fig. 5 with Fig. 6 shows that the search converges to the optimum location found by traditional load-pull simulations, and the final PAE values compare well between the search (44.93%) and the traditional load-pull simulation (45.87%).

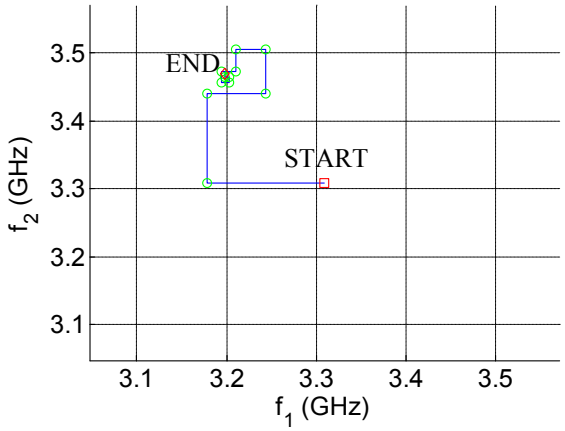

Fig. 4. Resonant frequency search simulation results with starting location $f_1 = 3.31$ GHz and $f_2 = 3.31$ GHz. An optimum PAE = 44.93% was found at $f_1 = 3.42$ GHz and $f_2 = 3.11$ GHz.

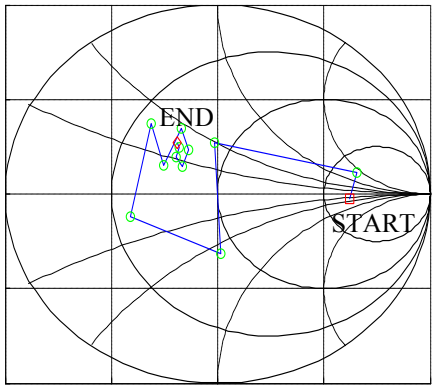

Fig. 5. Smith chart search trajectory for Fig. 4 search with starting location $f_1 = 3.31$ GHz and $f_2 = 3.31$ GHz

The simulation was performed at a non-central starting location within the search ranges to test the robustness of the search. In this case, the search still performs interval halving with the endpoint using the same methods, although the intervals on either side of the candidate with the endpoints are not necessarily identical. Figure 7 shows the resonant frequency mapping of a search initiated at $f_1 = 3.18$ GHz and $f_2 = 3.18$ GHz. The search converges to a similar PAE value of 41.14% at $f_1 = 3.42$ GHz and $f_2 = 3.11$ GHz. In this case, the end values for resonant frequencies are almost opposite of those shown in Fig. 4. This shows that different resonant frequency combinations can map to similar values of the load reflection coefficient Γ_L. By comparing Fig. 8 to Fig. 5, however, it is observed that both searches converge to the same Γ_L although the end resonant frequencies differ.

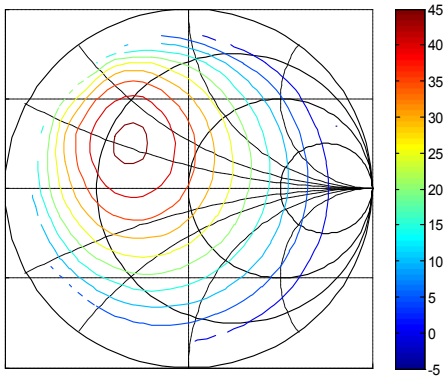

Fig. 6. PAE traditional load-pull results. The maximum PAE is 45.87% at $\Gamma_L = 0.45\angle 150°$.

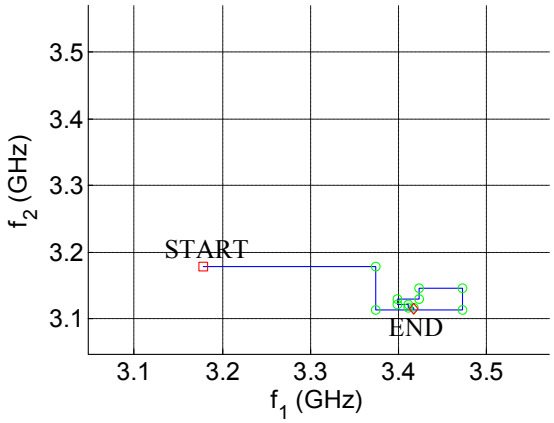

Fig. 7. Simulation results with starting location $f_1 = 3.18$ GHz and $f_2 = 3.18$ GHz. An optimum PAE = 41.14% was found at $f_1 = 3.42$ GHz and $f_2 = 3.11$ GHz.

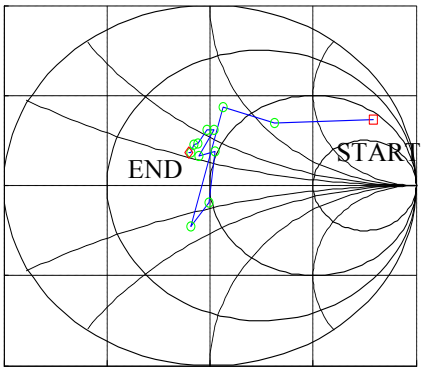

Fig. 8. Smith chart search trajectory of Fig. 7 search with starting location $f_1 = 3.18$ GHz and $f_2 = 3.18$ GHz with end PAE = 41.14%

For the search shown in Figures 7 and 8, the optimum PAE was found to be over 4 percent lower than the traditional load-pull results. An examination of the data shows that the alternating interval-halving approach can often miss an optimum due to the fact that the algorithm removes half of the remaining part of each frequency range at each step. As such, the optimum may not be reached if the steepest-ascent direction is not aligned along either the f_1 or f_2 axis in the resonant frequency plane. These results prompt the possibility that a gradient search may provide better accuracy and could be examined as a next step in the research process. However, the results obtained will allow the amplifier to operate relatively close to the optimum, and this is expected to occur in most cases.

V. Conclusions

A fast optimization for tuning the resonant frequencies in a high-power, reconfigurable evanescent mode cavity tuner to maximize power-added efficiency of a transistor has been presented. The results presented in this paper demonstrate the feasibility of this fast optimization for on-the-fly tuning of the reconfigurable network in reconfigurable radar applications. Directly tuning the resonant frequencies avoids the need for a characterization look-up (of the mapping between resonant frequencies and reflection coefficient) during tuning. This approach could amount to a significant reconfiguration time savings in practice.

Acknowledgment

This work has been funded by the Army Research Laboratory (Grant No. W911NF-16-2-0054). The views and opinions expressed do not necessarily represent the opinions of the U.S. Government. The authors are appreciative to Keysight Technologies for cost-free loan of the Advanced Design System software and to John Clark of the Army Research Laboratory for his helpful comments in writing this paper.

References

[1] H.M. Nemati *et al.*, "Design of Varactor-Based Tunable Matching Networks for Dynamic Load Modulation of High Power Amplifiers," *IEEE Transactions on Microwave Theory and Techniques,* Vol. 57, No. 5, May 2009, pp. 1110-1118.

[2] D. Qiao *et al.*, "An Intelligently Controlled RF Power Amplifier with a Reconfigrable MEMS-Varactor Tuner," *IEEE Transactions on Microwave Theory and Techniques*, Vol. 53, No. 3, Part 2, March 2005, pp. 1089-1095.

[3] W. du Plessis and P. Abrie, "Lumped Impedance Matching Using a Hybrid Genetic Algorithm," *Microwave and Optical Technology Letters*, Vol. 37, No. 3, pp. 210-212, May 2003.

[4] Z. Hays *et al.*, "Real-Time Amplifier Optimization Algorithm for Adaptive Radio Using a Tunable-Varactor Matching Network," 2017 IEEE Radio and Wireless Symposium, Phoenix, Arizona, January 2017.